# Mechanical Properties of Clay-Reinforced Polyamide

**K. MASENELLI-VARLOT,[1] E. REYNAUD,[2] G. VIGIER,[2] J. VARLET[3]**

[1]Laboratoire de Chimie du Solide Minéral, Université Henri Poincaré-Nancy I, BP 239, Vandœuvre-les-Nancy Cedex 54506, France

[2]INSA de Lyon, GEMPPM bâtiment 502, 20 avenue Albert Einstein, Villeurbanne Cedex 69621, France

[3]Rhodia Recherches CRL, 85 rue des frères Perret, BP 62, Saint-Fons Cedex 69192, France

*Received 24 April 2001; revised 30 October 2001; accepted 6 November 2001*

**ABSTRACT:** Intercalated and exfoliated nanocomposites were prepared by extrusion and injection of polyamide-6 and highly swollen or slightly swollen montmorillonite, respectively. The microstructure of the nanocomposites has been studied previously. In this article, we investigated the influence of the preferential orientation of the montmorillonite sheets on the mechanical properties of the nanocomposites. Dynamic mechanical analysis and tensile tests showed that the elastic modulus depends mainly on the filler loading. A parallel coupling could well account for the behavior of the nanocomposites. The calculated elastic and storage moduli of montmorillonite were set to 140 and 40 GPa, respectively. Compression tests were performed to study the anisotropy of the mechanical properties. The elastic modulus and flow strain were sensitive to the filler orientation. A Tandon–Weng approach was applied to consider the geometry of the filler. In all low-deformation tests, no significant difference between intercalated and exfoliated systems was observed. Finally, the influence of the dispersion and exfoliation state of the filler on the ultimate properties of the nanocomposites (tensile tests) is discussed. © 2001 John Wiley & Sons, Inc. J Polym Sci Part B: Polym Phys 40: 272–283, 2002

**Keywords:** nanocomposites; montmorillonite; mechanical properties; microstructure

## INTRODUCTION

Composite materials are widely used in various fields, such as automotive, aeronautics, and communications. Depending on the composite nature and structure, many of the following properties can be improved: hardness, tenacity, deformation temperature, price, and so forth. Nanocomposites refer to composites where one of the components has at least one dimension of the order of a few nanometers. They are a relatively new class of materials. The nanoscale dispersion gives better stiffness (influence of the length scale of the component phases). A few articles detail the advantages of using nanocomposites.[1]

Polymer/montmorillonite nanocomposites are very interesting because they are cheap, and the structure and chemistry of montmorillonite allow us to expect good mechanical properties. Montmorillonite is a natural inorganic material. Its general chemical formula is $(OH)_4Si_8(Al_{4-x}Mg_x)O_{20}$. Montmorillonite exhibits a crystalline structure, described by two-dimensional layers, that are composed of two tetrahedral sheets of silica surrounding an octahedral sheet of alumina or magnesia. Its chemical structure and interaction with the polymer is described in the literature.[2] An

*Correspondence to:* K. Varlot (E-mail: karine.varlot@lcsm.uhp-nancy.fr)

Journal of Polymer Science: Part B: Polymer Physics, Vol. 40, 272–283 (2002)

DOI 10.1002/polb.10088

ammonium-based organic surfactant is often used to modify the montmorillonite/polymer interactions. The intercalation of the polymer between montmorillonite sheets depends on the surfactant structure and especially the length of the carbon chain.[3,4] Three types of microstructure can be obtained.[5] Montmorillonite and the polymer can form immiscible phases. This case is not of great interest because it is not a real nanocomposite. In the exfoliated system, single sheets of montmorillonite are dispersed in the polymer matrix. The system is called "intercalated" when one or a few polymer chains are intercalated between montmorillonite sheets. The sheets remain relatively close to each other. A basal spacing can still be defined.

The mechanical properties of polymer/montmorillonite nanocomposites are outlined in the literature,[6,7] but very few articles focus on the way the microstructure can rule the mechanical properties of the nanocomposites. It is generally accepted that the exfoliated systems give better mechanical properties than intercalated ones,[8] but what "better mechanical properties" means has to be defined precisely.

We examined polyamide-6/montmorillonite nanocomposites. The specimens we used were injected because we wanted to be close to industrial processes. To explain the mechanical properties of such nanocomposites, we previously studied their microstructure. The main results have been published elsewhere.[9] We show that the montmorillonite sheets preferentially orient themselves around the injection axis. As far as exfoliated systems are concerned, an average distance between the montmorillonite sheets could be calculated from small-angle X-ray scattering (SAXS) spectra. Surprisingly, we could consider that the sheets are parallel to each other and uniformly distributed in the sample. Montmorillonite also played a major role in the crystallization of the polyamide-6 matrix. Montmorillonite prevents the crystallization in the $\alpha$ phase and promotes crystallization in the $\gamma$ phase. $\gamma$ Lamellae are expected to grow on the montmorillonite sheets. A recent article clearly shows the radial orientation of polyamide-12 lamellae relative to the montmorillonite sheets.[10]

In this article, we focus on the mechanical properties of polyamide/montmorillonite nanocomposites and we describe how the mechanical properties depend on the orientation of the montmorillonite sheets and the polyamide lamellae. First, we explain the low-deformation properties under a dynamic solicitation, traction, and compression. The results are confronted with laws of mixtures that consider the anisotropic microstructure of the nanocomposites. We then present the ultimate properties of the nanocomposites. Attention is particularly paid to their dispersion and exfoliation states.

## EXPERIMENTAL CONDITIONS

The clay was supplied by Southern Clay Products. Two of the following different surface treatments were mainly used: a slightly swollen montmorillonite (basal spacing $d_{001}$ = 18 Å) and a highly swollen one ($d_{001}$ = 36 Å). The surfactants used were methyl octadecyl bis-2-hydroxyethyl ammonium methylsulfate and dimethyl dioctadecyl ammonium chloride, respectively. The exchange ratio was 120 meq/100 g. However, other surfactants were used to determine the behavior of various exfoliated systems under traction. The characteristics of the composites are summarized in Table I.

As far as the elaboration of the composites is concerned, the controlled clay content was 5%. In fact, the mineral content is different because the clay contains a high proportion of surfactant. For example, in the case of the slightly swollen montmorillonite, the organic content is about 46% (ash content ca. 53%, water content ca. 1%). The actual concentration of montmorillonite was determined by weighing the samples before and after heating and burning at 800 °C for 2 h. The measurements were 2.7% for the highly swollen montmorillonite and 3.4% for the slightly swollen montmorillonite. The small difference was not expected to play a great role in the microstructure of the nanocomposites. However, as far as the mechanical properties are concerned, a correction is needed to consider the mineral content.

The composites were elaborated through the extrusion–injection route. The melt incorporation was performed with a double Leistritz double-screw extruder (diameter 34 mm, controlled temperature 250 °C). The samples were then injection moulded with a Demag 80 device (1053167 dumbells). In the following discussion, pure polyamide-6 (i.e., without montmorillonite) is called PA1. The nanocomposites generated from polyamide-6 and 5% highly swollen montmorillonite or 5% slightly swollen montmorillonite are called PA2 and PA3, respectively. Previous observations

**Table I.** Samples Used for the Tensile Tests

| Name | Surfactant | Exfoliation State | Dispersion State | Montmorillonite Content (wt %) |
|---|---|---|---|---|
| PA1 | — | — | — | 0 |
| PA2 | Dimethyl, dioctadecyl ammonium chloride | Intercalated | Good | 1.7 |
| | Dimethyl, dioctadecyl ammonium chloride | Intercalated | Good | 2.7 |
| | Dimethyl, dioctadecyl ammonium chloride | Intercalated | Very poor | 2.7 |
| PA3 | Methyl, octadecyl, bis-2-hydroxyethyl ammonium methylsulfate | Exfoliated | Poor | 2.4 |
| | Methyl, octadecyl, bis-2-hydroxyethyl ammonium methylsulfate | Exfoliated | Poor | 3.4 |
| PA4 | Methyl, octadecyl, bis-2-hydroxyethyl ammonium methylsulfate | Exfoliated | Poor | 6.5 |
| | Aminododecanoic acid | Exfoliated | Poor | 4.2 |
| | Methyl, hydrogenated rapeseed, 2-ethylhexyl ammonium methylsulfate | Exfoliated | Poor | 3.7 |
| | Methyl, hydrogenated tallow, 2-ethylhexyl ammonium methylsulfate | Exfoliated | Good | 2.5 |
| | Methyl, hydrogenated tallow, 2-ethylhexyl ammonium methylsulfate | Exfoliated | Good | 3.8 |

have shown that PA2 was intercalated and PA3 was exfoliated.[9]

The mechanical properties are very sensitive to the water content in the nanocomposites. Water indeed acts as a plasticizer. We characterized the nanocomposites in severe conditions without any water. The samples were dried at 85 °C under vacuum for at least 12 h and then cooled down under vacuum. The mechanical tests were performed just after the drying procedure to avoid water sorption before the test.

A dynamical mechanical analysis was performed on the nanocomposites. The frequency of the torsion oscillations was set to 1 Hz. The temperature ranged from −100 to +150 °C. The deformation was about $10^{-4}$, which ascertains the characterization of the linear behavior of the viscoelastic properties.

Tensile tests were performed at room temperature on an MTS Adamel Lhomargy DY35 machine. The speed was set to 5 mm/min. The samples were International Organization for Standardization 14125 (length 80 mm; section 10 × 4 mm). Young's modulus was measured with an accuracy of 10%. The crack shapes were observed using a scanning electron microscope (SEM) JEOL 840ALGS after gold coating. The accelerating voltage was set to 15 kV to avoid charging. Chemical mapping was performed to detect montmorillonite agglomerates.

Compression tests were carried out on small cubes of nanocomposites (4 mm side length) on an INSTRON8561 machine (two compression plates). The compression speed was 0.5 mm/min. The cube was thought to be small enough to prevent buckling and casklike deformation.

## RESULTS AND DISCUSSION

### Low-Deformation Properties

#### *Tensile Tests*

Tensile tests were performed to determine if the incorporation of montmorillonite into polyamide follows a law of mixtures. For this experiment, we had many samples with various montmorillonite contents (see Table I). We sorted the samples by their exfoliation state. Although the montmorillonite was swollen with various surfactants, we only made the difference between intercalated and exfoliated systems.

Figure 1 displays the dependence of Young's modulus on the montmorillonite content. Young's modulus was measured from the tensile curves as the slope of the true strain curve at no deformation. Five tests were performed for each material. Each point on the figure refers to the average Young's modulus determined from all the tests.

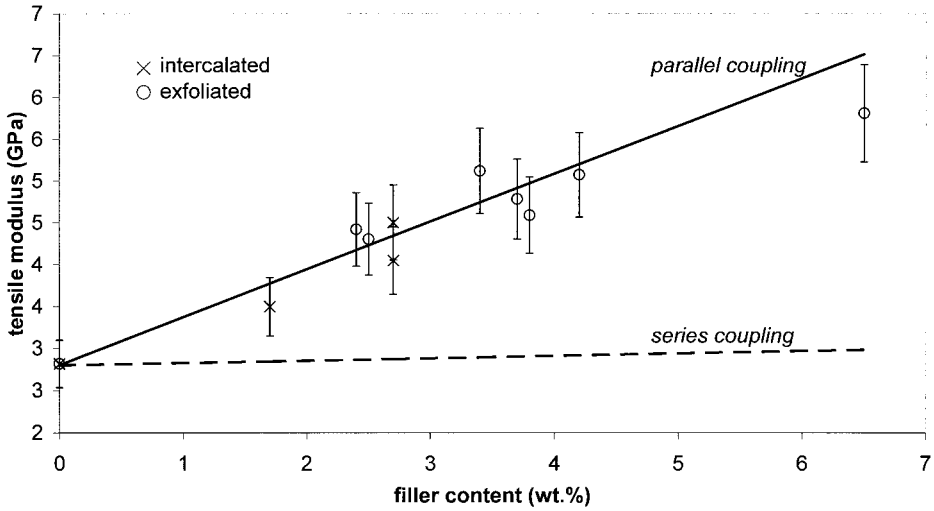


**Figure 1.** Young's modulus determined from tensile tests. A parallel coupling can well account for the behavior of both intercalated and exfoliated systems.

Young's modulus of pure polyamide-6 was 2.8 GPa. This value agrees with the literature, as far as dry polyamide-6 is concerned.[11] All the nanocomposites have a larger Young's modulus than pure polyamide-6. The reinforcement is larger for high filler loadings. The measurements show that Young's modulus increases linearly with the montmorillonite content. No significant difference can be made between intercalated and exfoliated systems.

To explain the increase of Young's modulus with the montmorillonite content, we used theoretical considerations on the basis of the moduli of the phases and the volume fraction of the filler. The simplest ways to describe a two-phase composite lead to the Reuss and Voigt bounds (also called rules of mixtures). The Voigt upper-bound (parallel coupling) formula corresponds to a laminate with the laminae aligned with the compressive load so that each phase experiences the same strain. The Reuss lower-bound (series coupling) structure is aligned perpendicular to the direction of load so that each phase experiences the same stress.

Because of the preferential orientation of the montmorillonite sheets relative to the deformation axis (see Fig. 2), the validity of the law of mixtures is analyzed. The linear dependence of Young's modulus on the filler loading suggests a parallel coupling (Voigt upper bound). The series coupling (Reuss lower bound) is displayed on the graph for comparison. Young's modulus of montmorillonite was set to 140 GPa and the density was equal to 2.3 $g \cdot cm^{-3}$, which are close to the values proposed in the literature.[12] From the orientation of the montmorillonite sheets as compared with the deformation axis, a mixed parallel series coupling should be used instead. The pileup of the montmorillonite sheets into tactoïds leads to the parallel part. The series contribution is due to the fact that the montmorillonite sheets are not as long as the sample but are separated from each other by polyamide. The tensile tests show that the series contribution can be neglected. The system reacts as though the montmorillonite sheets were endlessly long (Fig. 2). A possible explanation for this phenomenon can be given by the microstructure of the matrix. Therefore, the crystalline lamellae of the matrix (extra $\gamma$ phase) grown from the montmorillonite sheets could ensure the transfer of the load from one montmorillonite sheet to another.

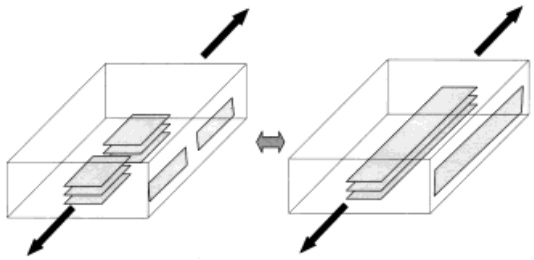

**Figure 2.** View of the applied deformation (tensile tests) as compared with the preferential orientation of the montmorillonite sheets.

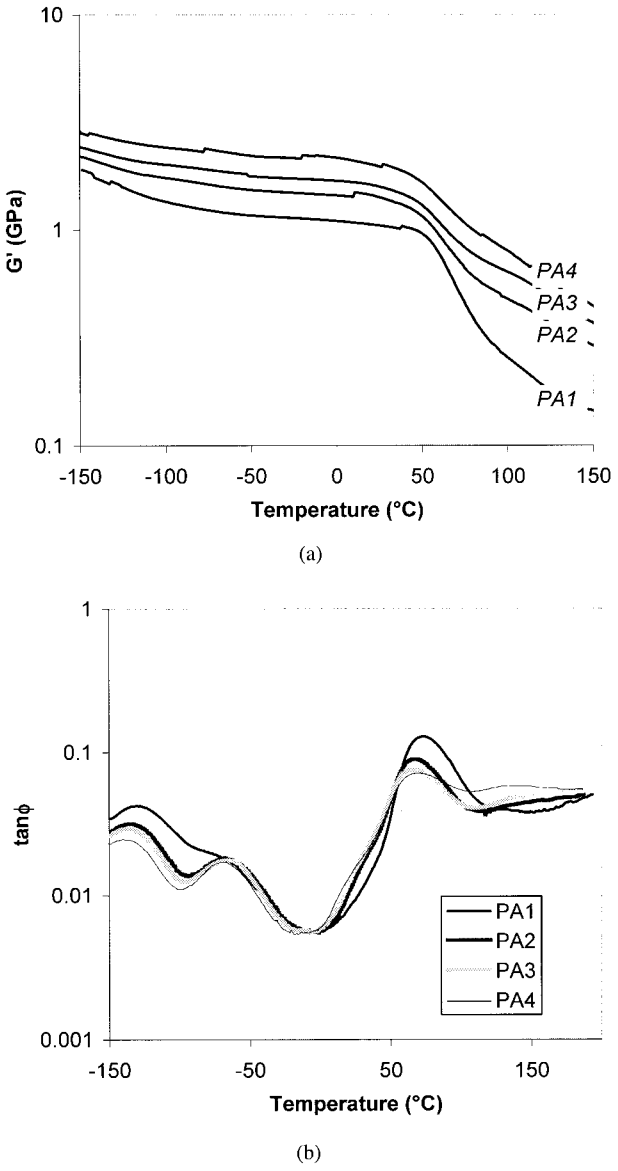


**Figure 3.** (a) Storage modulus and (b) loss factor of pure polyamide-6, PA2 (intercalated system) and PA3 (exfoliated system). A reinforcement of the storage modulus can be observed upon incorporation of montmorillonite.

## Dynamic Mechanical Analysis

Figure 3 shows the storage modulus and the loss factor of PA2 and PA3 as compared with pure polyamide-6 (PA1). A third nanocomposite, called PA4, was also included. It is similar to PA3 but contains 6.5 wt % slightly swollen montmorillonite instead of 3.4 wt % for PA3. It was examined to consider the different filler loading between PA2 and PA3. Generally speaking, the addition of montmorillonite modifies the response of the materials. First, the temperature of the main relaxation ($\alpha$), determined from $G''$, is shifted toward lower temperatures. The values are summarized in Table II. All the nanocomposites have the same relaxation temperature (60 °C), about 5 °C less than the temperature of pure polyamide-6 (65 °C). To explain the downshift of the main relaxation temperature, we measured the values of the glass temperatures by DSC. We observed that upon addition of montmorillonite, the glass temperatures were also shifted toward lower temperatures, by about 10 °C. The downshift of the glass temperature was assigned to the presence of surfactant (plasticizing effect). This may explain the decrease of the composites' main relaxation temperature. Another physical phenomenon may also participate to the latter shift. The loss factor reflects the way the various system components are sharing the deformation energy provided to the whole composite structure. The filler geometry, their orientation, and the particular crystalline structure they induce may be responsible for a mechanical coupling between the different phases within the composite that could give rise to the noted deviation from the matrix behavior.[13]

Moreover, the addition of montmorillonite increases the system storage modulus, as illustrated in Figure 3, which displays the variations of this modulus between −100 and +150 °C. From the raw data, the reinforcement is larger in an exfoliated system (PA3) than in an intercalated one (PA2). Yet the montmorillonite contents in PA2 and PA3, determined by weighing before and after burning, are different. For two temperatures, −50 °C, which is a typical temperature at which polyamide-6 is in the vitreous state, and +150 °C, which is characteristic of the rubbery plateau, the storage modulus varies linearly with the montmorillonite content. At the same time, the main relaxation peak has a lower intensity. This can be directly related to the increase of the storage modulus.

Because Young's modulus varies accordingly with the law of mixtures (parallel coupling), we checked the validity domain of this law during dynamic mechanical analysis. At −50 °C, $G'$ varies linearly with the filler loading (see Fig. 4). The parameters of the linear fit lead to a storage modulus of montmorillonite equal to about 40 GPa. Although no value could be found in the literature on the storage modulus of montmorillonite, 40 GPa is not an inconsistent value if we consider that it is roughly the third of the elastic modulus calculated from the tensile tests (140 GPa). Thus,

**Table II.** Characteristics of the Nanocomposites Undergone to a Dynamic Mechanical Analysis (Glass Temperature Was Measured by DSC)

| Name | Surfactant | Montmorillonite Content (wt %) | $T_\alpha$ (°C) | $T_g$ (°C) | $G'_{-50°C}$ (GPa) | $G'_{+150°C}$ (GPa) |
|---|---|---|---|---|---|---|
| PA1 | — | 0 | 65 | 55 | 1.17 | 0.14 |
| PA2 | Intercalated nanocomposite dimethyl dioctadecyl ammonium chloride | 2.7 | | 47 | 1.53 | 0.29 |
| PA3 | Exfoliated nanocomposite methyl octadecyl bis-2-hydroxyethyl ammonium methylsulfate | 3.4 | 60 | 46 | 1.78 | 0.36 |
| PA4 | Exfoliated nanocomposite methyl octadecyl bis-2-hydroxyethyl ammonium methylsulfate | 6.5 | | 46 | 2.21 | 0.44 |

we can consider that a parallel coupling can account for the dynamic properties of the nanocomposites in the vitreous state. This also agrees with the preferential orientation of the montmorillonite sheets determined previously by SAXS.[9] The schematic view of the applied deformation as compared with the orientation of the montmorillonite sheets is illustrated in Figure 5. As during the tensile tests, we would have expected to use a law of mixtures including both parallel and series couplings. It seems logical to consider a parallel coupling because the sample is viewed as a stack of concentric rings (polyamide and montmorillonite, alternatively). However, a series coupling should have been included to consider the polyamide that binds two montmorillonite sheets inside a ring. The linear dependence of the storage modulus on the montmorillonite content suggests that these areas containing polyamide can be neglected, suggesting that the load can be transferred from one sheet to another, maybe by the $\gamma$ lamellae of the matrix. This agrees with the interpretation of the behavior of the nanocomposites during the tensile tests.

At +150 °C, the storage modulus of the nanocomposites also varies linearly with the filler

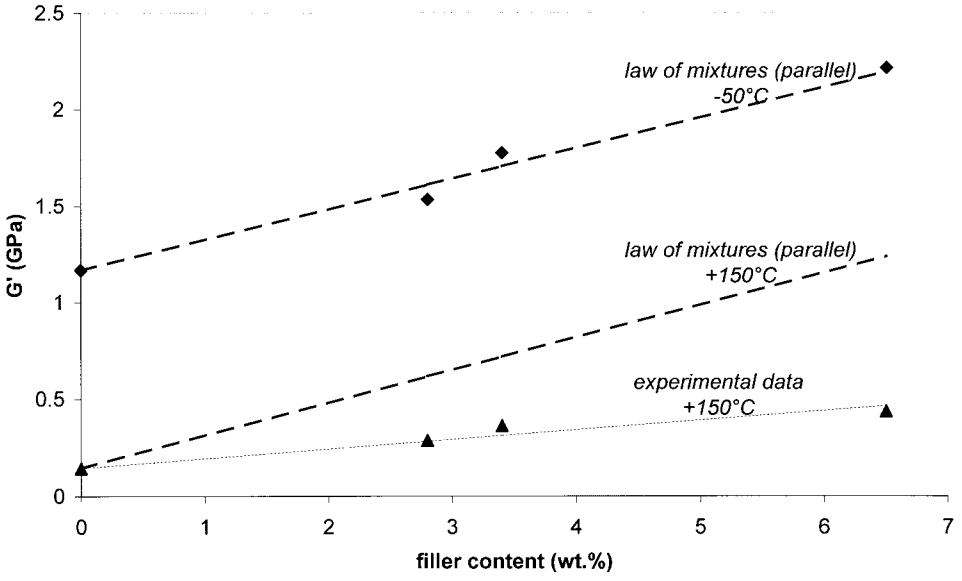


**Figure 4.** Dependence of the storage modulus on the filler loading. Two temperatures were chosen. At −50 °C, the matrix is in the vitreous state, and +150 °C lies on the rubbery plateau. There is a good agreement with the law of mixtures (parallel coupling). No difference was made between intercalated and exfoliated systems.

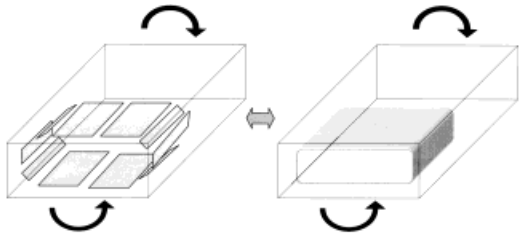

**Figure 5.** View of the applied deformation (dynamic mechanical analysis) as compared with the preferential orientation of the montmorillonite sheets.

loading. However, when assuming that the storage modulus of montmorillonite remains unchanged when increasing the temperature, we find that a parallel coupling cannot account for the properties of the nanocomposites (see Fig. 4). The calculated slope is far larger than the experimental slope. At −50 °C, a parallel coupling was consistent because in the vitreous state, crystalline and amorphous polyamides have almost the same mechanical characteristics (order of magnitude of the storage modulus: 1 GPa). At +150 °C, the amorphous polyamide becomes rubbery (≈1 MPa), whereas the properties of crystalline polyamide remain unchanged (≈1 GPa). In the vitreous state (−50 °C), a two-phase model can be applied, with montmorillonite on the one hand and polyamide on the other hand. On the rubbery plateau, a two-phase model should be nonvalid, and a three-phase model should rather be applied to consider the following microstructure of the polyamide matrix: montmorillonite, crystalline, and amorphous polyamides. Because montmorillonite promoted crystallization of PA-6 in the $\gamma$ phase, a lot of $\gamma$ lamellae are expected to grow on the montmorillonite sheets.[9] Thus, a self-coherent model where the filler is embedded into an interphase in which properties corresponds to that of crystalline PA-6 may well account for the experimental data.

### Compression Tests

Because of the shape of the nanocomposite samples, it was not possible to perform dynamic mechanical analysis and the tensile tests with various deformation axes. As far as the compression experiments are concerned, it was possible to study the influence of the montmorillonite orientation by choosing the deformation axis. Figure 6 displays a schematic view of the deformation axis as compared with the preferential orientation of

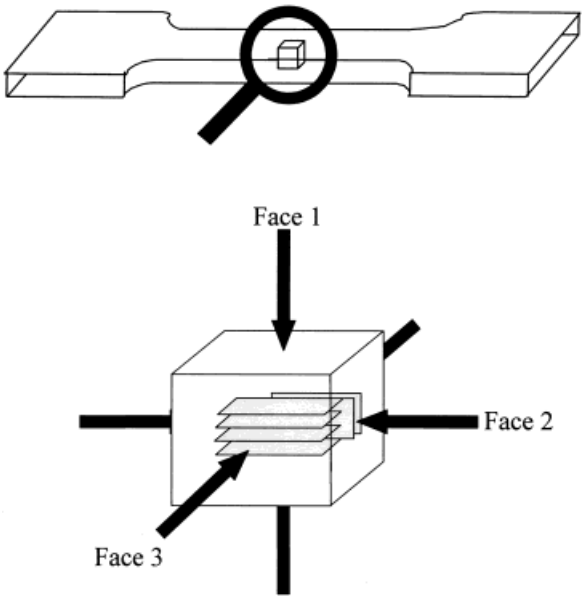


**Figure 6.** View of the deformation axes during the compression experiment as compared with the preferential orientation of the montmorillonite sheets.

montmorillonite. From the tensile tests and dynamic mechanical analysis, we can consider that montmorillonite forms a continuous phase in the direction of face 2 and face 3, respectively.

The values of the modulus and the flow strain are summarized in Table III. Only four samples were investigated. PA1 refers to pure polyamide-6. As expected, PA1 is an isotropic material. All three faces led to the same modulus and flow strain. As illustrated in Figure 7, the highest reinforcement in the composites is observed on face 2, the others leading to roughly similar values at the same filler loading. With respect to the morphological characterization, testing the composite in direction 2 consists of stressing material domains where the mechanical coupling between phases is of the parallel type (which is the upper

**Table III(a).** Modulus of the Nanocomposites Undergone to a Compression Test (MPa)

| | Montmorillonite Content (wt %) | Modulus (MPa) | | |
|---|---|---|---|---|
| | | Face 1 | Face 2 | Face 3 |
| PA1 | 0 | 1180 | 1224 | 1178 |
| PA2 | 2.7 | 1406 | 1494 | 1487 |
| PA3 | 3.4 | 1523 | 1897 | 1455 |
| PA4 | 6.5 | 1433 | 2077 | 1698 |

**Table III(b).** Flow Stress of the Nanocomposites Undergone to a Compression Test (MPa)

| | Montmorillonite Content (wt %) | Flow Stress (MPa) | | |
|---|---|---|---|---|
| | | Face 1 | Face 2 | Face 3 |
| PA1 | 0 | 79 | 85 | 84 |
| PA2 | 2.7 | 100 | 109 | 98 |
| PA3 | 3.4 | 105 | 135 | 110 |
| PA4 | 6.5 | 96 | 141 | 104 |

possible bound for mechanical coupling). Along directions 1 and 3, the tested domains are both of the parallel and series mechanical couplings that lower the modulus reinforcement, as experimentally observed.

To consider the aspect ratio of the montmorillonite sheets and explain the behavior of the nanocomposites along the three directions, use was made of the Tandon and Weng approach.[14] The major hypothesis of this approach is the following geometry of the filler: the montmorillonite sheets are considered as a disk that aspect ratio $\alpha$, defined as the ratio between the thickness and the diameter of the sheet, is set to 0.015 accordingly to the morphological characterization (thickness of a sheet: 0.7 nm; mean length: 50 nm).[9] Young's modulus and Poisson's coefficient of the montmorillonite are taken from the literature and are set to 170 GPa and 0.2, respectively. The model is also applied to spherical fillers (aspect ratio $\alpha = 1$) for comparison (see Fig. 7). The Tandon–Weng approach gives different properties of the composite according to the deformation axis. Nevertheless, along all directions the montmorillonite sheets lead to a larger reinforcement than spherical fillers.

As far as PA3 is concerned, the value chosen for the aspect ratio (0.015) can well account for the observed increase of the modulus along direction 2. Under our conditions, the representative elementary volume of the composite exactly corresponds to a disk of clay embedded in a polyamide matrix. Along directions 1 and 3, the experimental values are always slightly larger than the calculated values. The representative elementary volume is more complicated than that considered by the model, undoubtedly because the montmorillonite sheets tend to coil themselves around the injection axis.

The experimental behavior of PA4 is obviously different from the model prediction. Such a deviation has already been mentioned in the literature when increasing the filler content in a composite elaborated from plasma desorption mass spectrometry and clay.[12] The researchers consider that the higher the filler loading, the less perfect the interfacial bound. From transmission electron microscopic observations, percolation cannot occur. Nevertheless, the nature, shape, and orientation of the montmorillonite sheets can lead to a possible anisotropy of the crystalline phase. The differences between the model and the experimental values could therefore be explained by the fact that the model does not consider the crystalline structure of the matrix.

The intercalated composite (PA2) shows a weaker reinforcement effect along direction 2. The experimental values are indeed lower than the upper boundary defined by the Tandon–Weng approach. The representative elementary volume cannot be smaller than a tactoïd. However, the montmorillonite sheets are weakly bound to each other inside a tactoïd, and the distances between the tactoïds are large. The mechanical coupling would therefore be weaker in intercalated composites than in exfoliated systems.

## Ultimate Properties (Tensile Tests)

The ultimate properties of the composites are summarized in Table IV. To compare them, it is necessary to get information on the montmoril-

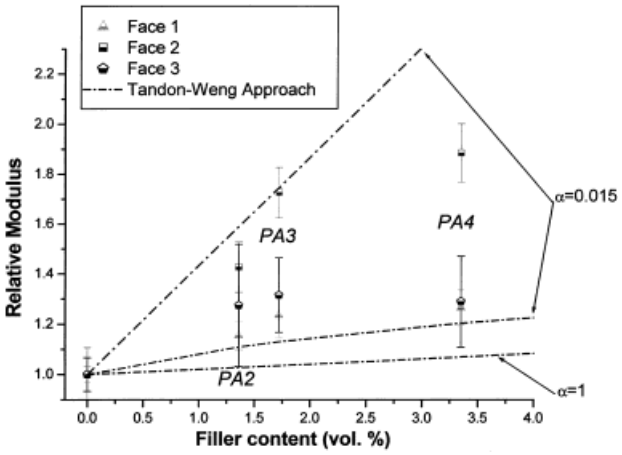


**Figure 7.** Dependence of the elastic modulus on the filler loading during compression experiments. The nanocomposites show anisotropic properties. The largest reinforcement is obtained with face 2, which agrees with the preferential orientation of the montmorillonite sheets.

**Table IV.** Characteristics of Various Nanocomposites Undergone to a Tensile Test (Information Regarding the Montmorillonite Dispersion Was Included To Compare the Failure Strains)

| Name | Surfactant | Exfoliation State | Dispersion State | Montmorillonite Content (wt %) | Young's Modulus (MPa) | Flow Strain | Flow Stress (MPa) | Failure Strain | Failure Stress (MPa) |
|---|---|---|---|---|---|---|---|---|---|
| PA1 | — | — | — | 0 | 2816 | 0.028 | 77 | 0.618 | 98 |
| | Dimethyl, dioctadecyl ammonium chloride | Intercalated | Good | 1.7 | 3497 | 0.026 | 90 | 0.154 | 65 |
| PA2 | Dimethyl, dioctadecyl ammonium chloride | Intercalated | Good | 2.7 | 4048 | 0.022 | 87 | 0.067 | 78 |
| | Dimethyl, dioctadecyl ammonium chloride | Intercalated | Very poor | 2.4 | 3629 | 0.024 | 82 | 0.105 | 81 |
| | Methyl, octadecyl, bis-2-hydroxyethyl ammonium methylsulfate | Exfoliated | Poor | 2.4 | 4420 | — | — | 0.027 | 95 |
| PA3 | Methyl, octadecyl, bis-2-hydroxyethyl ammonium methylsulfate | Exfoliated | Poor | 3.4 | 5121 | — | — | 0.026 | 95 |
| PA4 | Methyl, octadecyl, bis-2-hydroxyethyl ammonium methylsulfate | Exfoliated | Poor | 6.5 | 5813 | — | — | 0.010 | 65 |
| | Methyl, hydrogenated tallow, 2-ethylhexyl ammonium methylsulfate | Exfoliated | Good | 2.5 | 4253 | — | — | 0.029 | 96 |

lonite content, the exfoliation state, and the dispersion state. Dispersion is very important information because failure can be induced on agglomerates. Several materials have been examined to compare the influence of the filler loading, dispersion, and exfoliation states.

Several trends can be deduced from the tensile tests on the nanocomposites. First, all the nanocomposites have worse failure characteristics than pure polyamide-6. The best elongation at break was obtained on the intercalated systems containing 1.7 wt % montmorillonite and was four times lower than the elongation at break of pure polyamide-6. The influence of the filler loading on the failure characteristics can be deduced from Table IV. As far as intercalated systems are concerned, the incorporation of montmorillonite clearly increases the flow stress and failure stress but decreases the corresponding stains. The samples become harder but more fragile. All the exfoliated samples were brittle (no flow characteristics). The failure shifts toward lower strains when increasing the filler loading. There is no corresponding increase of the failure stress. This may be due to the fact that the exfoliated samples have a lot of montmorillonite agglomerates that facilitate the failure by initiating the cracks (lower stress and lower strain).

The influence of the dispersion on failure is dependent on the surfactant. The intercalated systems were obtained with a hydrophobic surfactant, whereas a polar surfactant was used to obtain the exfoliated systems with a poor dispersion. To draw a comparison with the exfoliated systems, we elaborated intercalated systems with a poor dispersion by using a single-screw extruder. It appeared that all the characteristics, except the failure strain, were independent of the dispersion in the intercalated systems. The failure was even observed at larger strains with the poorly dispersed samples. The characterization of the failure shapes gave interesting insight. The increase of the failure strain was attributed to the disappearance of shear bands. Shear bands were the main cause of failure for the intercalated sample with 2.7 wt % montmorillonite (PA2). They were created on the remaining montmorillonite agglomerates. The poorly dispersed intercalated sample had more agglomerates that would have caused more shear bands. The observation of the failure shapes by SEM revealed that decohesion occurred at the interface between polyamide and all the montmorillonite agglomerates (see Fig. 8). The decohesion was possible because the hydrophobic surfactant led to a weak interface (no hydrogen bonding between polyamide and the surfactant). After the decohesion, the sample was equivalent to a sample without any montmorillonite agglomerates. Moreover, the relaxation of the stress was possible by means of the cavities created after the decohesion process.[15]

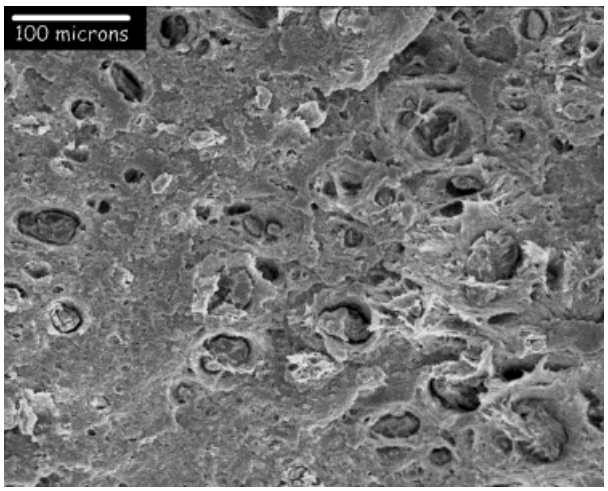


**Figure 8.** : SEM micrograph of the intercalated sample with a poor dispersion after the tensile test. Decohesion occurred at the interfaces between polyamide and the montmorillonite agglomerates.

Even with a poor dispersion, the intercalated systems have a larger failure strain than exfoliated systems. This can be directly attributed to the chemical structure of the surfactant. The exfoliated systems (PA3 and PA4) were elaborated with a polar surfactant. The polar groups allow hydrogen bonding between the polymer chains and the surfactant molecules, leading to a strong interface. Figure 9 displays the SEM analysis of each part of the failure shape in the case of PA3 (exfoliated system with 3.4 wt % montmorillonite). The montmorillonite agglomerates are visible through the mapping of aluminium and silicon. The failure initiated on a lot of montmorillonite agglomerates. The agglomerates were detected on each part of the failure shape. This means that the crack initiated on and propagated inside the agglomerates, which agrees with the literature.[10] No decohesion at the interfaces was observed.

Finally, intercalated and exfoliated systems were elaborated with a good dispersion and a similar montmorillonite content (2.7 and 2.5 wt %, respectively). As expected from the parallel coupling, we can consider that Young's moduli are similar. On the contrary, the failure characteris-

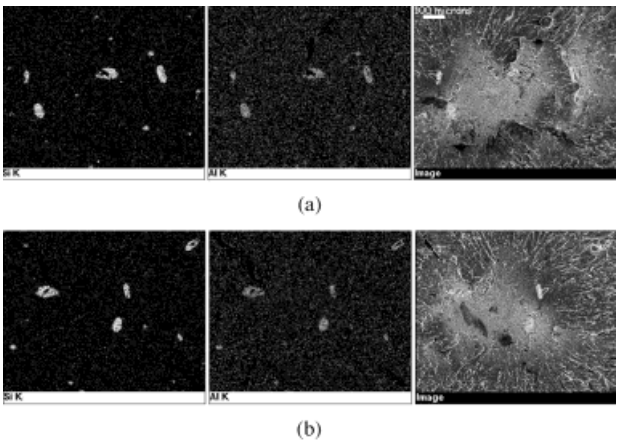


**Figure 9.** Mapping of aluminium and silicon on each part of the failure shape of PA3. The failure was initiated on a lot of montmorillonite agglomerates. No decohesion at the interfaces between polyamide and the agglomerates was observed. (scale bar: 100 microns)

tics are very different. The exfoliated system has a larger failure stress but a lower failure strain. This suggests that the largest failure stresses can be obtained with exfoliated systems, but large failure strains will be more easily attainable with intercalated systems. However, further experiments are needed because the ductile-to-brittle transition seems to occur at filler loadings between 2.5 and 7.5 wt %.[16]

## CONCLUSION

We elaborated on nanocomposites from polyamide-6 and montmorillonite via an extrusion–injection route. We previously studied the microstructure of the nanocomposites. In this article, we focused on the mechanical properties of the nanocomposites and related them to the microstructure. The reinforcement effect of montmorillonite was observed in dynamic mechanical analysis, tensile, and compression tests.

The storage and Young's moduli were mainly dependent on the filler loading. A parallel coupling could well account for their variations. This is consistent with the preferential orientation of the montmorillonite sheets. When assuming a density close to 2.35 g.cm$^{-3}$, the Young's and storage moduli of the montmorillonite were calculated to be equal to 140 and 40 GPa, respectively. Young's modulus was relatively in agreement with the values proposed in the literature. From the parallel coupling, we could consider that there is an efficient load transfer, probably because of the crystalline structure of the matrix (presence of extra $\gamma$ lamellae, grown perpendicularly to the montmorillonite sheets), and that the system reacts as though montmorillonite formed continuous concentric cylinders centered on the injection axis.

The main relaxation temperature of the nanocomposites was shifted toward lower temperatures as compared with polyamide-6. This was mainly attributed to a decrease of the glass temperature. The influence of a mechanical coupling between montmorillonite and polyamide-6 on the main relaxation temperature was also discussed.

As far as the compression experiments are concerned, several deformation directions could be analyzed. The reinforcement depended on the orientation of the montmorillonite sheets. The largest reinforcement was obtained when compressing the nanocomposites along a direction parallel to the injection axis. A Tandon–Weng approach was used to consider the aspect ratio of the montmorillonite sheets. It could account for the behavior of the exfoliated system containing 3.4 wt % montmorillonite. The other composites exhibited lower moduli. This phenomenon was discussed in light of their microstructures.

Finally, the ultimate properties were determined from tensile tests. We found that the dispersion, the montmorillonite content, and the chemical structure of the surfactant played major roles on the failure properties of the nanocomposites. When comparing exfoliated and intercalated samples, which have the same level of dispersion and montmorillonite content, we suggested that the largest failure stresses could be obtained with the exfoliated systems, whereas the intercalated systems could lead to the largest failure strains.

## REFERENCES AND NOTES

1. Yamashita, A.; Takahara; A. Compos Interfaces 1999, 6, 247–258.
2. Giannelis, E. P.; Krishnamoorti, R.; Manias, E. Adv Polym Sci 1999, 138, 107–147.
3. Vaia, R. A.; Giannelis, E. P. Macromolecules 1997, 30, 7990–7999.
4. Lan, T.; Kaviratna, P. D.; Pinnavaia, T. J. Chem Mater 1995, 7, 2144–2150.
5. Lyatskaya, Y.; Balazs, A. C. Macromolecules 1998, 31, 6676–6680.

6. Massam, J.; Pinnavaia, T. J. Mater Res Soc Symp Proc 1998, 520, 223–232.
7. Jimenez, G.; Ogata, N.; Kawai, H.; Ogihara, T. J Appl Polym Sci 1997, 64, 2211–2220.
8. Kojima, Y.; Usuki, A.; Kawasumi, M.; Okada, A.; Fukushima, Y.; Kurauchi, T.; Kamigaito, O. J Mater Res 1993, 8, 1185–1189.
9. Varlot, K.; Reynaud, E.; Kloppfer, M. H.; Vigier, G.; Varlet, J. J Polym Sci Part B: Polym Phys 2001, 39, 1360–1370.
10. Kim, G. M.; Lee, D. H.; Hoffmann, B.; Kressler, J.; Stöppelmann, G. Polymer 2001, 42, 1095–1100.
11. Trotignon, J. P.; Verdu, J.; Dobracginsky, A.; Piperaud, M. Précis de matières plastiques. Structures-propriétés, mise en œuvre, normalisation. Nathan, Ed. Paris, 1996.
12. Shia, D.; Hui, C. Y.; Burnside, S. D.; Giannelis, E. P. Polym Compos 1998, 19(5), 608–617.
13. Cuillery, P. Viscoélasticité d'une structure métal / polymère/métal. Phénomènes d'interface, Ph.D. Thesis, INSA de Lyon, France, 1996.
14. Tandon, G. P.; Weng, L. T. Polym Compos 1984, 5(4), 327–333.
15. Bagheri, R.; Pearson, R. A. Polymer 1995, 36(25), 4883–4885.
16. Cho, J. W.; Paul, D. R. Polymer 2001, 42, 1083–1094.